Methodology for Identifying Soiling on PV Panels Using RGB Images and Deep Learning

Katerina Gabrovska-Evstatieva[1], Tsvetelina Kaneva[2], Irena Valova[3], Dimitar Trifonov[4], Nikolay Valov[5], Ventsislav Keseev[6], Nicolay Mihailov[7], Boris Evstatiev[8]
Faculty of Natural Science and Education, University of Ruse Angel Kanchev, Ruse 7004, Bulgaria [1]
Faculty of Electrical Engineering, Electronics and Automation,
University of Ruse Angel Kanchev, Ruse 7004, Bulgaria[2, 3, 4, 5, 6, 7, 8]

***Abstract*—Soiling is one of the major factors that can affect the performance of PV installations in many regions of the world. On the other hand, the variety of PV models, types of soiling, and climate conditions makes it very difficult to create a universal model. To address this problem, this study presents a methodology for the identification of soiling on PV panels via semantic segmentation, which can support the decision-making process in terms of surface cleaning and automation of the process. The methodology includes data collection, preparation of training and testing data, training of models, and application of the optimal one. Next, the methodology is demonstrated using a small dataset of clean and dirty PV panels, three neural network architectures (DeepLab v3, U-Net, and PSPNet), and two backbone models (ResNet34 and ResNet50). The obtained results show the feasibility of the methodology and allow highlighting the DeepLab v3 model with a ResNet34 backbone as the best-performing algorithm for identifying pigeon droppings. The second-best combination is the U-Net + ResNet34, which showed good efficiency for identifying smaller dirty areas. The proposed methodology could be useful for operators of large-scale photovoltaic installations by supporting the decision-making process when it comes to the timely cleaning of specific areas for performance improvement and lower costs.**

***Keywords*—PV soiling; semantic segmentation; pixel-based classification; neural network; RGB images**

I. Introduction

In times of energy crisis and a changing climate, the importance of renewable energy sources (RES) increases significantly. Out of them, photovoltaic (PV) systems are dominating the renewables market due to their versatility and low-maintenance requirements. Nevertheless, numerous factors exist that influence PV installations' performance and, as a result, open many opportunities for their optimization. Two of these factors are soiling and shading of the photovoltaic surface, which could have a great impact on a PV installation's performance [1,2]. They are known to lead to various consequences, such as reduced energy yield [3-5], increased panel degradation [5,6], hotspots [7], fire hazard [8,9], etc. In most situations, shading is a factor that can be acknowledged during design time, but there are limited options for its mitigation.

Soiling, on the other hand, could be effectively mitigated during exploitation; however, there are a number of factors to consider. According to [10], soiling accumulation can reduce energy production by up to 20%, depending on the environmental conditions. In [11] was obtained that agricultural soiling could reduce light transmission by up to 40% and the power output by up to 10%. Similar results about bird droppings showed that the power losses could reach a maximal value between 10% and 23%, depending on the month of the year and the PV installation location [12].

To mitigate the impact of soiling, different approaches for cleaning the photovoltaic surfaces exist. The most basic one is manual cleaning, which is known to be both expensive and time-consuming [13]. Furthermore, it requires water that is free from minerals to prevent the creation of spots and scale build-up. Other studies have suggested using the thrust of a drone to clean dust from the PV surface [14] or different types of robots moving over the PV surface [15,16]. In [17,18], a mechanism for self-cleaning panels' surface by removing dust particles using spherical water droplets is proposed, where a sliding or rolling motion is imparted. In all cases, the price is a major factor, and therefore, it is important to properly schedule the cleaning cycles [19]. The importance of properly deciding on when to clean the PV surface increases even more for building-integrated photovoltaics, where conventional cleaning approaches are rarely applicable [20].

Another problem is the type of soiling. Most of the above-mentioned studies propose solutions for removing dust. However, periodic cleaning, especially if a waterless method is used, is not always a suitable solution for bird droppings, which are especially common in the urban environment. All of this shows that the identification of bird droppings is a major factor for the optimization of the PV cleaning process.

Numerous studies have proposed a wide range of approaches for identifying soiling on PV surfaces based on image processing and classification [21], RGB image analysis [22], and pixel- and object-based identification. In [10], a methodology for the classification of RGB images of PV surfaces as either clean or dirty was proposed. The images were preliminarily processed using red channel doubling and conversion to multichannel, which allowed the dirty parts to be highlighted. Different machine learning algorithms were tested, and the best results were achieved by an artificial neural network, reaching an F1 score of 91.3%. In another study [23], deep learning was used to classify RGB images of PV modules into one of the 5 classes: very unclean, slightly unclean, medium clean, slightly clean, and clean. The optimal results

were achieved by the UTran neural network architecture with a ResNet50 backbone, reaching an accuracy of 96.41%.

In [24], a pixel-based classification approach was used to identify hotspots on PV surfaces by classifying the pixels of IR images using machine learning algorithms. The output of the models is a mask that identifies potential problems. A different approach was used in [25] with images in the visible spectrum, aimed at teaching a robot to identify and clean soiled surfaces automatically. The study proposed a threshold value used on the red channel of the RGB image in order to create the cleaning masks. In [26], several methods for semantic segmentation were used to generate soiling masks on PV surfaces. The algorithms used include Random Forest, XGBoost, LightGBM, and the U-Net neural network architecture. The neural network achieved the highest performance, reaching an accuracy and F1 score of 96.82% and 93.37%, respectively.

Other studies investigated the object-based approach for identifying soiling on PV panels. In [27], RGB images were used with the SDS-YOLO v5 architecture. The model achieved F1 scores of 0.700 and 0.781 for the bird droppings and dust classes, respectively. A similar approach was used in [28], where the YOLO v8 model's soiling identification efficiency exceeded 90%. In [29], different classification models were compared to identify PV performance degradation caused by dust and dirt accumulation. The results demonstrated the potential of data-driven approaches to improve the monitoring and maintenance of photovoltaic systems and to optimize energy efficiency.

A completely different approach was used in [30], where real-world meteorological and production data were used to develop and validate a predictive algorithm based on Stacked Ensemble Learning (SEL) and Decision Trees (DT). It achieved high accuracy in predicting soiling and panel performance, which shows that such models can help optimize maintenance and improve the energy efficiency of photovoltaic systems.

The performed analysis shows that numerous studies have proposed different approaches for the identification of soiling on PV surfaces with AI algorithms, with the object-based ones commonly having a lower accuracy compared to the pixel- and classification-based ones. Some of them achieved quite impressive results, yet their accuracy generally becomes lower when used on different datasets, which is normal for machine learning. The various PV technologies have different appearances in terms of color, cell dimensions, etc., which is a major limiting factor for the models to be more universal. Furthermore, the soiling factors also vary in different geographic locations. This means that in order to achieve optimal results, the models should be trained with a dataset that was obtained for a specific PV facility. Most studies concentrate on the modelling part, rather than the methodological aspects, which are more important as they allow for obtaining improved results for the local specifics. Therefore, this could be considered a research gap.

Considering the above-mentioned, this study aims to propose a methodology for assessing the soiling of PV panels, which allows for training high-accuracy deep learning models capable of supporting the decision-making process in terms of organizing the cleaning routines. The feasibility of the proposed methodology is demonstrated using a small dataset with PV modules under the impact of pigeon droppings, obtained from the region of Ruse, Bulgaria. The study also evaluates the performance of different deep learning architectures and backbone models for identifying bird droppings with different impact areas.

II. Materials and Methods

A. Methodology of the Study

The proposed methodology for assessing the condition of a PV surface is summarized in Fig. 1. It can be described in 4 steps as follows:

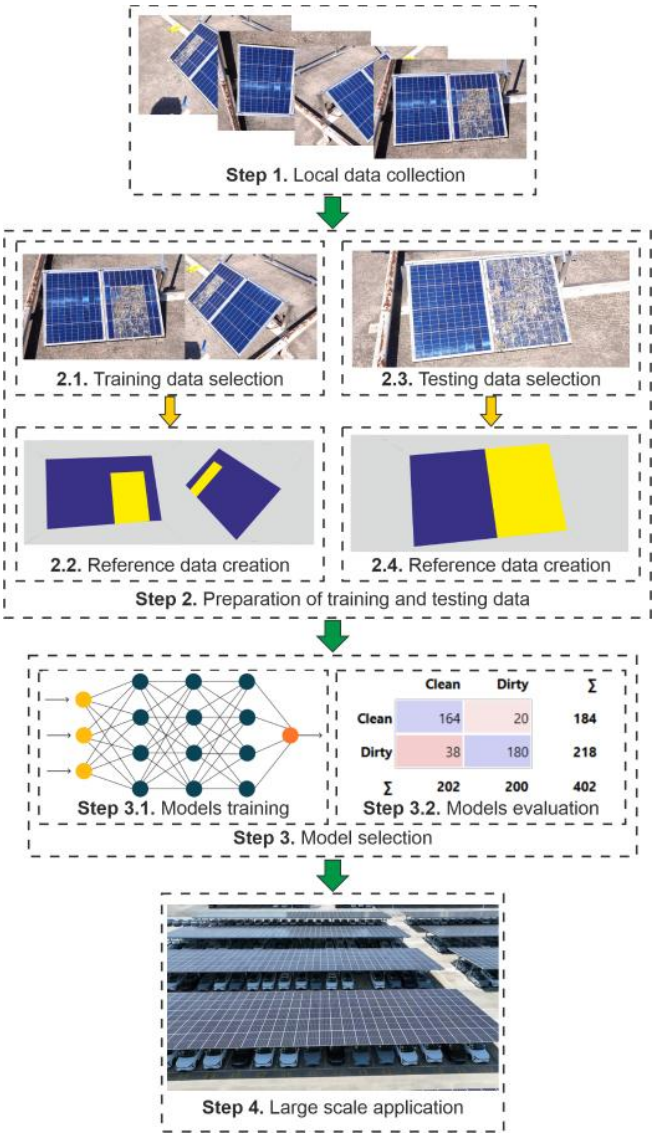

Fig. 1. Methodology for identification of soiling on a PV surface.

Step 1. Local data collection

This step includes the collection of images from the specific PV installation that is to be evaluated. The data must be obtained for the specific facility for several reasons:

- The way the panels look depends on their technology, weather conditions, etc., which is always site-specific;
- The potential soiling is also site-specific as it depends on the local soil types, the type of birds, etc.

Furthermore, when collecting the local dataset, it is recommended that the following requirements be met:

- It should represent all potential types of soiling on the PV surface;
- It should include surfaces of well-cleaned panels;
- It should include the different background surfaces available at the site (grass, concrete, etc.).

Step 2. Preparation of training and testing data

Next, training and testing data should be prepared, which is implemented in two similar processes.

1) Training data selection: In this phase, several images are selected from the local dataset, which represent all major situations, such as clean panels, panels with different types of soiling, and images with different types of surrounding backgrounds. It is recommended that the different situations are more or less equally represented in order to improve the performance of the models. According to the proposed methodology, the selected images should be merged into a single larger image.

2) Reference data creation: Next, using the compiled training image, reference data should be created. In this study, the following classes are used:

- Clean PV surface ("Clean") – an area of the PV surface, which is in good condition and no soiling can be observed;
- Dirty PV surface ("Dirty") – an area of the PV surface, on which soiling can be observed;
- Background ("Back") – everything else that is not part of the PV surface (whether clean or dirty) is considered a surrounding or background area.

If necessary, the "Dirty PV surface" class could be divided into subclasses, representing different types of soiling. However, in this study, we have only investigated soiling caused by bird droppings.

In this phase, the pixels of the compiled training image are manually classified into one of the selected categories. An important recommendation is that if the operator cannot clearly identify the class of a certain area of the image, the corresponding pixels should remain uncategorized.

3) Testing data selection: In this phase, other images should be selected for testing purposes that are different from the training ones. They should also adequately represent all common situations. Similarly, the images could be merged into a single testing image for easier processing and analysis.

4) Reference data creation: This phase is similar to 2.2 and includes classifying the pixels of the testing image into the adopted classes.

Step 3. Model selection

This step includes two phases – training models and evaluating their performance, aimed at identifying the optimal ones.

1) Models' training: In this study, three deep learning architectures are selected:

- U-Net- is widely used for pixel-based classification and has shown good performance for dust detection in photovoltaic panels [31]. It is also known for achieving high accuracy with fine details, being extremely efficient when working with small data sets, and typically requires less training time and hardware resources [32]. Despite being lighter and faster, it often performs relatively well compared to other models [33];
- DeepLab v3- is another semantic segmentation model, which is known to return good results with the identification of photovoltaic installations [34,35], surface soiling [36], hot-spot defects [37], etc. It usually returns better accuracy at different object scales and more complex images, but can be significantly slower to train and requires a larger amount of data and hardware resources [38];
- Pyramid Scene Parsing Network (PSPNet)- has also shown good results with PV panel identification [35]. It is known for better distinguishing objects based on analysis of the surrounding environment, but can be significantly slower to train and requires a larger amount of data and hardware resources, although some works report that it is the most efficient in terms of execution time [39].

Furthermore, for each one of them, two backbone models have been used: ResNet-34 and ResNet-50, thus making a total of 6 combinations. The difference between ResNet-34 and ResNet-50 lies mainly in their depth and architectural complexity. ResNet-34 is a lighter backbone model, requiring less training data for simpler tasks, training faster, and taking up less memory on the graphics processing unit. ResNet-50, on the other hand, is more complex and is better at recognizing fine textures and complex objects, but requires more data to avoid overfitting. Furthermore, it requires more computing power and memory, and training takes longer.

This phase of the methodology includes training the models using the training data, prepared in phases 2.1 and 2.2 of the methodology.

2) Models' evaluation: Next, each of the trained models is applied to the testing data prepared in phases 2.3 and 2.4, and a classification image is created. Thereafter, the performance of each model is evaluated against the reference data using the following metrics:

- Accuracy – estimates the proportion of total correct predictions:

$$Acc = \frac{TruePositive+TrueNegative}{TruePositive+TrueNegative+FalsePositive+FalseNegative} \quad (1);$$

- Precision – estimates the share of true positives out of all positively identified pixels:

$$Precision = \frac{TruePositive}{TruePositive+FalsePositive} \quad (2);$$

- Recall – estimates the share of the correctly identified pixels:

$$Recall = \frac{TruePositive}{TruePositive+FalseNegative} \quad (3);$$

- F1 score – averages the precision and recall:

$$F1 = 2 \times \frac{Precision \times Recall}{Precision+Recall} \quad (4);$$

- Cohen's Kappa – evaluates the level of agreement between classified and reference data, with 0 corresponding to no agreement at all (all pixels were classified incorrectly) and 1 corresponding to perfect agreement (all pixels were classified correctly) [40].

The above metrics are used to select the best-performing model(s).

Step 4. Large-scale application

Once the best-performing model is selected, it can be used for large-scale identification of soiling at the specific photovoltaic facility as an instrument for automating the decision-making and cleaning processes.

B. Means of the Investigation

In this study, the software ArcGIS Pro v. 3.6.1 is used, developed by Esri Inc. Even though this tool was created as a GIS analysis instrument, it is also applicable to images that are not mapped to a specific coordinate system.

ArcGIS Pro provides a wide range of object- and pixel-based machine learning and deep learning algorithms, integrated tools for the creation of reference data, comparison between the modeled and reference data, generation of confusion matrices, estimation of different measures, etc. Furthermore, all of the above is implemented in a friendly graphical user interface, i.e., no specialized programming knowledge and skills are required. This means that with appropriate instructions, the ArcGIS Pro tool could be used by operators of photovoltaic installations without the need for IT-specific qualifications.

C. Organization of the Experiment

The experiment in this study was performed at the site of PV Park Kanev, located in the University of Ruse "Angel Kanchev", Ruse, Bulgaria, geographic coordinates 43.85344121491259, 25.969174955358763 (Fig. 2). Two 50W polycrystalline PV panels with model CL-SM50P were used in the experiment. One of the two panels has been placed on the floor of a dovecote for two weeks. This allowed its surface to be densely covered with pigeon droppings, which are one of the main sources of PV soiling in the Bulgarian urban landscape.

Fig. 2. Location of the experimental site.

III. Results and Discussion

In this section, the study aims to demonstrate the feasibility of the proposed methodology using a limited amount of input data. The clean and dirty PV panels were installed at the experimental site using a specially created mounting structure, and numerous images of them were made from different angles. Next, different areas of the soiled PV surface were gradually cleaned, and additional photos were made at each stage (Fig. 3). The data collection was finalized when both PV surfaces were clean.

Fig. 3. Photos of the two PV panels with different levels of dirtiness.

Next, according to Step 2 of the methodology, four images were selected, which represent different aspects of the experimental situation, such as:

- The PV modules are photographed from different angles, which represent the surfaces differently affected by the solar rays;

- The surrounding area is observed from different angles, which influences its view, the impact of shadows, etc.

The four images were merged into a single one using Microsoft's MS Paint tool. Thereafter:

- The prepared training image was imported into ArcGIS Pro v. 3.6.1;
- Reference areas were created for the three classes (Clean, Dirty, and Background) with the Image Classification tool using polygons (Fig. 4a).

Finally, the created reference data was exported in the "Classified tiles" metadata format with X/Y tile size 256 and X/Y Stride 128. Similarly, four testing images were selected, merged into a single image, and reference data was created for it (Fig. 4b).

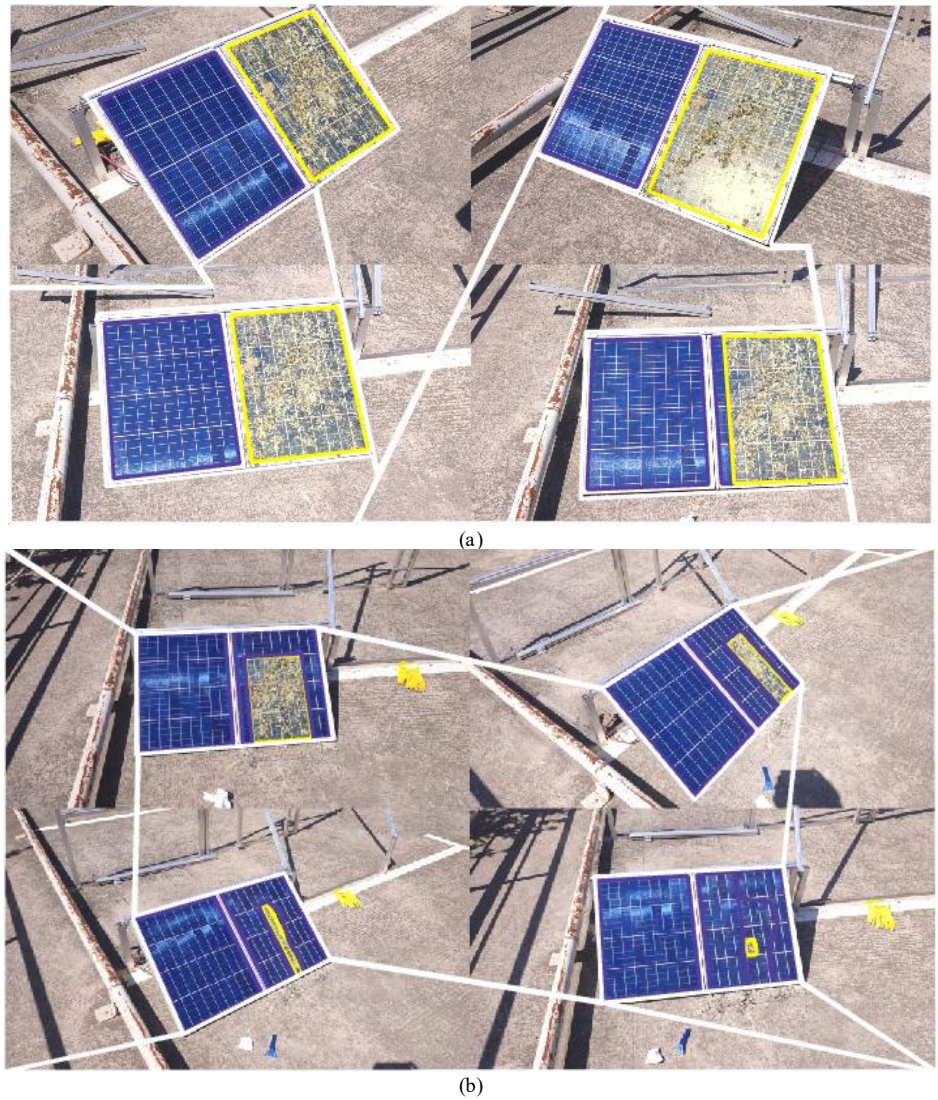

(a)

(b)

Fig. 4. The selected training (a) and testing (b) images with the marked reference polygons.

Following Step 3 of the methodology, 6 models were trained using the three NN architectures and the two backbone models on an HP Pavilion laptop with an NVidia GeForce MX350 GPU. 20 epochs were used for the training, 10% of the input data was used for validation, the optimal learning rate was automatically extracted from the learning curve, and all other parameters were kept at their default values. The obtained accuracies and F1 scores for the six models are summarized in Table I. It can be seen that if accuracy and F1 score are used as the main indicators, the DeepLabv3+ResNet50 combination is the worst-performing model. The differences between the measures of the other 5 models are 1-2 thousandths, and therefore could be considered insignificant. In general, the U-Net and PSPNet-based models achieve the highest performance.

On the other hand, when the Kappa coefficient is used, the PSPNet-based models have the lowest performance, while the U-Net+ResNet34 combination is the second best. The DeepLabv3+ResNet34 achieved the best performance, reaching a Kappa score of 0.996. It is important to mention that Cohen's Kappa is considered a more stable indicator than Accuracy because it excludes the chance of hitting the result when some data predominates [41].

TABLE I. SUMMARY OF THE SIX MODELS' TRAINING SCORES

№	Model	Accuracy	F1 Score	Kappa
1	DeepLab v3 + ResNet34	0.982	0.987	0.996
2	DeepLab v3 + ResNet50	0.975	0.980	0.985
3	U-Net + ResNet34	0.983	0.987	0.988
4	U-Net + ResNet50	0.984	0.988	0.980
5	PSPNet + ResNet34	0.983	0.987	0.954
6	PSPNet + ResNet50	0.983	0.988	0.962

The conclusion from the measures analysis is that the DeepLab v3+ResNet34 model, even though requiring more resources and time, could perform slightly better, especially in situations such as the current one, when comparatively little data is available. U-Net+ResNet34 is expected to perform about the same, but with less required time and resources. However, according to [42], DeepLabV3+ outperforms U-Net in terms of both speed and accuracy.

Next, the six models were applied to the testing image, and the obtained classification images are presented in Fig. 5. At first glance, it can be seen that all models perform very well, though some false positives can be observed. Furthermore, it can be observed that larger dirty areas are well identified by all models, while the results with smaller and thinner ones are more variable, and some false positives and false negatives can be observed.

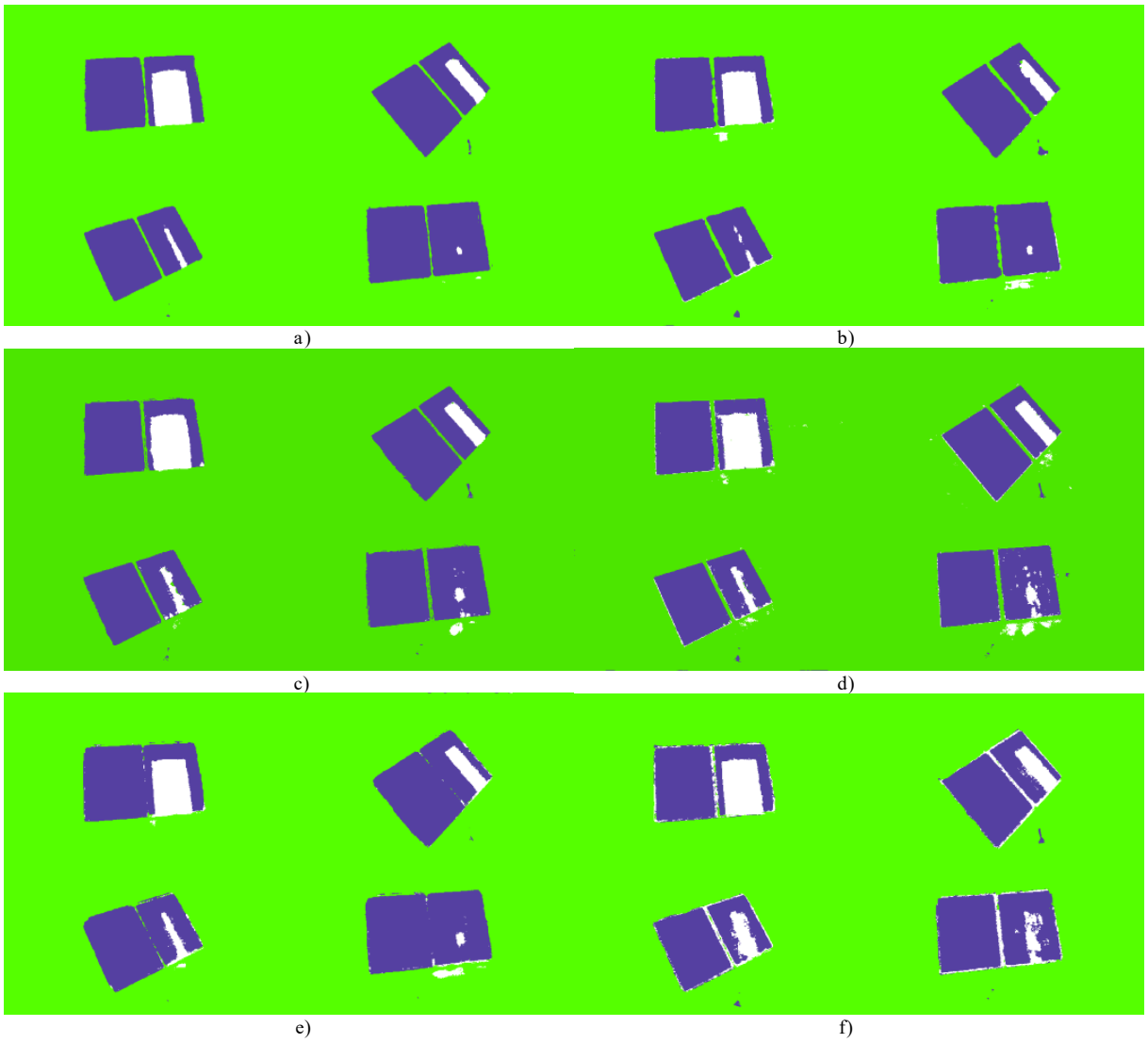

Fig. 5. Classification results for the testing image done with: DeepLab v3 + ResNet34 (a); DeepLab v3 + ResNet50 (b); U-Net + ResNet34 (c); U-Net + ResNet50 (d); PSPNet + ResNet34 (e); PSPNet + ResNet50 (f).

To get a better understanding of the models' performances, they were assessed using the "Accuracy assessment" tool in ArcGIS, 10,000 randomly selected pixels, and the Stratified random strategy was used on the reference testing data to generate the confusion matrices for the six situations.

The results for the DeepLab v3 + ResNet34 model are presented in Table II. It can be seen that the model has almost perfect performance, with an average F1 score of 0.999. The lowest precision and recall are obtained for the Dirty class, reaching values of 0.974 and 0.993, respectively, which indicates the classification of some false positives.

TABLE II. CONFUSION MATRIX AND MEASURES FOR THE TESTING DATA WITH THE DEEPLAB V3 + RESNET34 MODEL

		Predicted				Metrics		
		Clean	***Dirty***	***Back***	***Total***	***Prec.***	***Rec.***	***F1***
Actual	***Clean***	1332	4	5	1341	0.999	0.993	0.996
	Dirty	0	149	1	150	0.974	0.993	0.983
	Back	1	0	8508	8509	0.999	1.000	1.000
	Total	**1333**	**153**	**8514**	**10000**	**0.999**	**0.999**	**0.999**

Table III presents the performance of the DeepLab v3 + ResNet50 model. Its metrics are slightly lower for the clean and background classes, as for the dirty class, the precision and recall have dropped significantly, reaching values of 0.902 and 0.890, resulting in an F1 score of 0.896.

TABLE III. CONFUSION MATRIX AND MEASURES FOR THE TESTING DATA WITH THE DEEPLAB V3 + RESNET50 MODEL

		Predicted				Metrics		
		Clean	***Dirty***	***Back***	***Total***	***Prec.***	***Rec.***	***F1***
Actual	***Clean***	1330	14	6	1350	0.999	0.985	0.992
	Dirty	0	138	17	155	0.902	0.890	0.896
	Back	1	1	8490	8492	0.997	1.000	0.999
	Total	1331	153	8513	9997	0.996	0.996	0.996

Next, in Table IV and Table V, the measures for the two U-Net models are shown. Unlike the DeepLab models, these achieved higher precision for the dirty class, reaching up to 1.000 with the ResNet50 backbone; however, the recall is lower, which indicates an increased share of false positives. These results confirm the classification images in Fig. 5, which also show the identification of many false-positive "dirty" pixels.

TABLE IV. CONFUSION MATRIX AND MEASURES FOR THE TESTING DATA WITH THE U-NET + RESNET34 MODEL

		Predicted				Metrics		
		Clean	***Dirty***	***Back***	***Total***	***Prec.***	***Rec.***	***F1***
Actual	***Clean***	1320	0	10	1330	0.990	0.992	0.991
	Dirty	13	154	7	174	0.994	0.885	0.936
	Back	0	1	8495	8496	0.998	1.000	0.999
	Total	1333	155	8512	10000	0.997	0.997	0.997

TABLE V. CONFUSION MATRIX AND MEASURES FOR THE TESTING DATA WITH THE U-NET + RESNET50 MODEL

		Predicted				Metrics		
		Clean	***Dirty***	***Back***	***Total***	***Prec.***	***Rec.***	***F1***
Actual	***Clean***	1311	0	3	1314	0.986	0.998	0.992
	Dirty	19	153	30	202	1.000	0.757	0.862
	Back	0	0	8481	8481	0.996	1.000	0.998
	Total	1330	153	8514	9997	0.995	0.995	0.994

Finally, in Table VI and Table VII, the results for the PSPNet models are summarized. Similarly to the U-Net models, the dirty class precision is 1.000, which indicates that all dirty pixels were correctly identified. However, the recall decreases even more, reaching 0.748 and 0.698 with the ResNet34 and ResNet50 backbones, respectively. Once again, this indicates that these models return too many false positives when it comes to the dirty areas of the PV panel, which might lead to misleading results and have a significant impact on the decision-making process.

TABLE VI. CONFUSION MATRIX AND MEASURES FOR THE TESTING DATA WITH THE PSNET + RESNET34 MODEL

		Predicted				Metrics		
		Clean	***Dirty***	***Back***	***Total***	***Prec.***	***Rec.***	***F1***
Actual	***Clean***	1325	0	71	1396	0.993	0.949	0.971
	Dirty	9	154	43	206	1.000	0.748	0.856
	Back	0	0	8400	8400	0.987	1.000	0.993
	Total	1334	154	8514	10002	0.988	0.988	0.987

TABLE VII. CONFUSION MATRIX AND MEASURES FOR THE TESTING DATA WITH THE PSNET + RESNET50 MODEL

		Predicted				Metrics		
		Clean	***Dirty***	***Back***	***Total***	***Prec.***	***Rec.***	***F1***
Actual	***Clean***	1300	0	33	1333	0.975	0.975	0.975
	Dirty	33	155	34	222	1.000	0.698	0.822
	Back	0	0	8447	8447	0.992	1.000	0.996
	Total	1333	155	8514	10002	0.990	0.990	0.989

The obtained results show that the DeepLab v3 model with a ResNet34 backbone achieved the best performance, followed by the U-Net + ResNet34 one, for the following reasons:

- All models achieved more or less similar performance for the clean and background classes, with their precisions/recalls varying between 0.975 and 1.000;
- Most models achieved great precision for the dirty class, varying between 0.974 and 1.000 (the only exception is the DeepLab v3 + ResNet50 model, which achieved a precision of 0.902);
- The DeepLab v3 + ResNet34 model achieved the highest recall for the dirty class, reaching a value of 0.993, while this measure for all other models is significantly lower, ranging between 0.698 and 0.890.

These results also correspond with those obtained using the Kappa coefficient during the training phase. They confirm that Cohen's Kappa is a more reliable measure and could be used as the main indicator for selecting the optimal model.

IV. CONCLUSION

The current study presents a methodology for the identification of soiling on PV panels, which is optimized for providing reliable site-specific results. It can be used as a supporting instrument in the decision-making process of cleaning large photovoltaic installations. The methodology includes data collection, preparation of training and testing

data, training of models, and identification of the optimal one, which can then be applied on a large scale.

Next, the feasibility of the methodology is demonstrated by using limited experimentally obtained data from the PV park Kanev, Ruse, Bulgaria. An image dataset was created with clean and dirty PV panels under the impact of pigeon droppings. Training and testing images were selected, and reference data were created for them using three classes: "clean", "dirty", and "background". Three deep learning architectures were used: DeepLab v3, U-Net, and PSPNet. Furthermore, each one of them was trained with the ResNet34 and ResNet50 backbones. All trained models achieved more or less similar metrics and very good performance.

However, after they were applied to a testing dataset, the DeepLab v3 model with a ResNet34 backbone showed the highest performance, expressed in the best ratio between precision and recall regarding the "dirty" class. The second-best combination is the U-Net + ResNet34, which proved to be extremely efficient when working with small datasets. Both models could be applied in practice for the identification of soiling areas with relatively small datasets specific to the photovoltaic site. The study results also showed that Cohen's Kappa could be used as the main indicator for selecting the optimal model of the methodology, which is an important observation for the future application of the methodology.

The methodology proposed in this study could be useful for operators of large photovoltaic installations by supporting the decision-making process when creating the cleaning schedule. Even though the obtained results are quite promising, they have some limitations. They were not tested with real data, obtained from drones or satellites, which is an important goal for future research. Furthermore, it is worth investigating the possibility of increasing the performance of all algorithms by using a secondary model for limiting the analyzed area only to the area of PV modules, thus allowing the removal of the "background" class.

ACKNOWLEDGMENT

This study is financed by the European Union—NextGenerationEU through the National Recovery and Resilience Plan of the Republic of Bulgaria, project no. BGRRP-2.013-0001.

REFERENCES

[1] J. A. Tsanakas et al., "Assessment of Soiling Dynamics and Cleaning Efficiency for Photovoltaic Modules Under Different Dust Environments," Solar RRL, vol. 10, no. 6, Dec. 2025, doi: 10.1002/solr.202500792.

[2] R. K. Pachauri et al., "Impact of Partial Shading on Various PV Array Configurations and Different Modeling Approaches: A Comprehensive Review," in IEEE Access, vol. 8, pp. 181375-181403, 2020, doi: 10.1109/ACCESS.2020.3028473.

[3] Y. Mhanni and Y. Lagmich, "Maximizing Solar Panel Efficiency in Partial Shade: The Improved POA Solution for MPPT," International Journal of Advanced Computer Science and Applications, vol. 15, no. 3, 2024, doi: 10.14569/ijacsa.2024.0150397.

[4] M. R. Maghami, H. Hizam, C. Gomes, M. A. Radzi, M. I. Rezadad, and S. Hajighorbani, "Power loss due to soiling on solar panel: A review," Renewable and Sustainable Energy Reviews, vol. 59, pp. 1307–1316, Jun. 2016, doi: 10.1016/j.rser.2016.01.044.

[5] M. J. Alshareef, "A Comprehensive Review of the Soiling Effects on PV Module Performance," in IEEE Access, vol. 11, pp. 134623-134651, 2023, doi: 10.1109/ACCESS.2023.3337204.

[6] K. G. Gabrovska-Evstatieva, D. T. Trifonov, and B. I. Evstatiev, "A Review of the Key Factors Influencing the Performance of Photovoltaic Installations in an Urban Environment," Electricity, vol. 6, no. 2, p. 23, May 2025, doi: 10.3390/electricity6020023.

[7] M. Bressan, A. Gutierrez, L. Garcia Gutierrez, and C. Alonso, "Development of a real-time hot-spot prevention using an emulator of partially shaded PV systems," Renewable Energy, vol. 127, pp. 334–343, Nov. 2018, doi: 10.1016/j.renene.2018.04.045.

[8] Z. Wu, Y. Hu, J. X. Wen, F. Zhou, and X. Ye, "A Review for Solar Panel Fire Accident Prevention in Large-Scale PV Applications," in IEEE Access, vol. 8, pp. 132466-132480, 2020, doi: 10.1109/ACCESS.2020.3010212.

[9] A. Lysyi, A. Sachenko, P. Radiuk, M. Lysyi, and O. Savenko, "Enhanced fire hazard detection in solar power plants: an integrated UAV, AI, and SCADA-based approach," RADIOELECTRONIC AND COMPUTER SYSTEMS, vol. 2025, no. 2, pp. 99–117, May 2025, doi: 10.32620/reks.2025.2.06.

[10] B. I. Evstatiev, D. T. Trifonov, K. G. Gabrovska-Evstatieva, N. P. Valov, and N. P. Mihailov, "PV Module Soiling Detection Using Visible Spectrum Imaging and Machine Learning," Energies, vol. 17, no. 20, pp. 5238–5238, Oct. 2024, doi: 10.3390/en17205238.

[11] P. Gebhardt, P. Katouli, T. Kaltenbach, T. Bretzel, L.-M. Bieber, I. Haedrich, "EVALUATING THE IMPACT OF SOILING ON AGRIVOLTAIC SYSTEMS," European Photovoltaic Solar Energy Conference and Exhibition 2025, 2025, available online: https://publica-rest.fraunhofer.de/server/api/core/bitstreams/82384218-ec05-4370-9fe7-7b6e292e0b9c/content.

[12] A. K. Sisodia, "Effect of bird dropping deposition on photovoltaic (PV) module performance at different sites," International Journal of Science and Research Archive, vol. 13, no. 2, pp. 3569–3573, Dec. 2024, doi: 10.30574/ijsra.2024.13.2.2566.

[13] S. Gochhait, R. Asodiya, T. Hasanmani, V. Patin, and O. Maslova, "Application of IoT: A Study on Automated Solar Panel Cleaning System," 2022 4th International Conference on Electrical, Control and Instrumentation Engineering (ICECIE), Kuala Lumpur, Malaysia, 2022, pp. 1-4, doi: 10.1109/ICECIE55199.2022.10000375.

[14] S. Rehman, M. A. Mohandes, A. E. Hussein, L. M. Alhems, and A. Al-Shaikhi, "Cleaning of Photovoltaic Panels Utilizing the Downward Thrust of a Drone," Energies, vol. 15, no. 21, p. 8159, Nov. 2022, doi: 10.3390/en15218159.

[15] S. A. O. Sanya, M. Houngbedji, M. F. O. Sanya, and D. C. Akowanou, "Design of a Robotic System for Cleaning Solar Panels in Benin," Open Journal of Applied Sciences, vol. 15, no. 04, pp. 962–975, 2025, doi: 10.4236/ojapps.2025.154065.

[16] G. Ashtaputre and A. Bhoi, "Artificial Intelligence Based Solar Panel Cleaning Robot," vol. 14, pp. 12–15, 2019, doi: 10.9790/2834-1403021215.

[17] X. Gong and S. He, "Highly Durable Superhydrophobic Polydimethylsiloxane/Silica Nanocomposite Surfaces with Good Self-Cleaning Ability," ACS Omega, vol. 5, no. 8, pp. 4100–4108, Feb. 2020, doi: 10.1021/acsomega.9b03775.

[18] S. Maharjan et al, "Self-cleaning hydrophobic nanocoating on glass: A scalable manufacturing process," Materials Chemistry and Physics, vol. 239, p. 122000, Jan. 2020, doi: 10.1016/j.matchemphys.2019.122000.

[19] M. Rashid, M. Yousif, Z. Rashid, A. Muhammad, M. Altaf, and A. Mustafa, "Effect of Dust Accumulation on the Performance of Photovoltaic Modules for Different Climate Regions," Heliyon, vol. 9, no. 12, pp. e23069–e23069, Dec. 2023, doi: 10.1016/j.heliyon.2023.e23069.

[20] S. Umar et al., "A building integrated solar PV surface-cleaning setup to optimize the electricity output of PV modules in a polluted atmosphere," Renewable Energy, vol. 216, pp. 119122–119122, Aug. 2023, doi: 10.1016/j.renene.2023.119122.

[21] U. Naeem, K. Chadda, S. Vahaji, J. Ahmad, X. Li, and E. Asadi, "Aerial Imaging-Based Soiling Detection System for Solar Photovoltaic Panel

Cleanliness Inspection," Sensors, vol. 25, no. 3, pp. 738–738, Jan. 2025, doi: 10.3390/s25030738.

[22] R. Cavieres, R. Barraza, D. Estay, J. Bilbao, and P. Valdivia-Lefort, "Automatic soiling and partial shading assessment on PV modules through RGB images analysis," Applied Energy, vol. 306, p. 117964, Jan. 2022, doi: 10.1016/j.apenergy.2021.117964.

[23] M. Li and Y. Wang, "Deep Learning for Dust Accumulation Analysis on Desert Solar Panels: A CNN-Transformer Approach," in IEEE Access, vol. 13, pp. 69857-69872, 2025, doi: 10.1109/ACCESS.2025.3561363.

[24] M. Abdelsattar, A. AbdelMoety, and A. Emad-Eldeen, "Applying Image Processing and Computer Vision for Damage Detection in Photovoltaic Panels," Mansoura Engineering Journal, vol. 50, no. 2, Mar. 2025, doi: 10.58491/2735-4202.3263.

[25] T. Pivem, F. de Oliveira de Araujo, L. de Oliveira de Araujo, and G. S. de Oliveira, "Application of a Computer Vision Method for Soiling Recognition in Photovoltaic Modules for Autonomous Cleaning Robots," Signal & Image Processing: An International Journal, vol. 10, no. 03, pp. 43–59, Jun. 2019, doi: 10.5121/sipij.2019.10305.

[26] T. Cruz-Rojas, J. A. Franco, Q. Hernandez-Escobedo, D. Ruiz-Robles, and J. M. Juarez-Lopez, "A novel comparison of image semantic segmentation techniques for detecting dust in photovoltaic panels using machine learning and deep learning," *Renewable Energy*, p. 119126, Aug. 2023, doi: 10.1016/j.renene.2023.119126.

[27] U. Naeem, K. Chadda, S. Vahaji, J. Ahmad, X. Li, and E. Asadi, "Aerial Imaging-Based Soiling Detection System for Solar Photovoltaic Panel Cleanliness Inspection," Sensors, vol. 25, no. 3, pp. 738–738, Jan. 2025, doi: 10.3390/s25030738.

[28] H. El Karch, R. El Gouri, Y. Natij, M. Benally, and A. Mezouari, "AI-Based Smart Real-Time PV Panels Soiling Recognizing System Using Deep Neural Network Framework on NVIDIA Jetson Nano Embedded GPU," Ingénierie des systèmes d'information, vol. 29, no. 5, pp. 1687–1699, Oct. 2024, doi: 10.18280/isi.290503.

[29] S. Selvi, V. Devaraj, and R. P. P.s, "Detection of Soiling on PV Module using Deep Learning," International Journal of Electrical and Electronics Engineering, vol. Volume 10, Jul. 2023, doi: 10.14445/23488379/IJEEE-V10I7P108.

[30] I. Radonjić, M. A. Amin, M. Petronijević, P. Tsankov, and M. Ćalasan, "Soiling identification and forecasting in urban environment," Engineering Science and Technology, an International Journal, vol. 71, p. 102188, Sep. 2025, doi: 10.1016/j.jestch.2025.102188.

[31] T. Cruz-Rojas, J. A. Franco, Q. Hernandez-Escobedo, D. Ruiz-Robles, and J. M. Juarez-Lopez, "A novel comparison of image semantic segmentation techniques for detecting dust in photovoltaic panels using machine learning and deep learning," Renewable Energy, p. 119126, Aug. 2023, doi: 10.1016/j.renene.2023.119126.

[32] T. Mostafid, "Tumor Segmentation with U-Net and DeepLabv3+: A Review," Medium, Jun. 13, 2024. https://medium.com/@t.mostafid/tumor-segmentation-with-u-net-and-deeplabv3-a-review-048e10001fb2.

[33] A. R. Agduma and R. Dein, "Multi-model convolutional neural network architectures for coastal forest extent and aboveground biomass estimation," Remote Sensing Applications Society and Environment, pp. 101647–101647, Jun. 2025, doi: 10.1016/j.rsase.2025.101647.

[34] M. Kleebauer, C. Marz, C. Reudenbach, and M. Braun, "Multi-Resolution Segmentation of Solar Photovoltaic Systems Using Deep Learning," Remote Sensing, vol. 15, no. 24, p. 5687, Jan. 2023, doi: 10.3390/rs15245687.

[35] X. Chao, L. Zhang, Y. Li, J. Nie, S. Yang, and S. Ercisli, "Optimization Method for Remote Sensing Image-Based Photovoltaic Panel Segmentation via Perception-Driven Enhancement in Nonideal Environments," in IEEE Journal of Selected Topics in Applied Earth Observations and Remote Sensing, vol. 18, pp. 22513-22529, 2025, doi: 10.1109/JSTARS.2025.3602477.

[36] E. Ka, S. Go, Ulziitamir Davaadorj, S. Choi, and A. Nasridinov, "Comparative Analysis of Deep Learning-Based Image Segmentation Models for Solar Panel Soiling Detection," MITA2022, Jul. 2022.

[37] Y. Lei, X. Wang, A. An, and H. Guan, "Deeplab-YOLO: a method for detecting hot-spot defects in infrared image PV panels by combining segmentation and detection," Journal of Real-Time Image Processing, vol. 21, no. 2, Mar. 2024, doi: 10.1007/s11554-024-01415-x.

[38] P. Choure and S. Prajapat, "Exploring U-Net, FCN, SegNet, PSPNet, Mask R-CNN and Using DeepLabV3+ for Multiclass Semantic Segmentation on Satellite Images of Western Ghats," Dec. 2025, doi: 10.22541/au.176479420.03812962/v1.

[39] A. Moghimi, M. Welzel, T. Celik, and T. Schlurmann, "A Comparative Performance Analysis of Popular Deep Learning Models and Segment Anything Model (SAM) for River Water Segmentation in Close-Range Remote Sensing Imagery," in IEEE Access, vol. 12, pp. 52067-52085, 2024, doi: 10.1109/ACCESS.2024.3385425.

[40] D. Sarkar, D. Guha, P. Tarafdar, S. Sarkar, A. Ghosh, and D. Dey, "A comprehensive evaluation of contemporary methods used for automatic sleep staging," Biomedical Signal Processing and Control, vol. 77, p. 103819, Aug. 2022, doi: 10.1016/j.bspc.2022.103819.

[41] M. Carpentier, C. Combescure, L. Merlini, and T. V. Perneger, "Kappa statistic to measure agreement beyond chance in free-response assessments," BMC Medical Research Methodology, vol. 17, no. 1, Apr. 2017, doi: 10.1186/s12874-017-0340-6.

[42] Herlawati and R. T. Handayanto, "Land Cover Segmentation of Multispectral Images Using U-Net and DeeplabV3+ Architecture," Jurnal Ilmu Komputer dan Informasi, vol. 17, no. 1, pp. 89–96, Feb. 2024, doi: 10.21609/jiki.v17i1.1206.